Complete bio-degradation of PBAT via evolved hydrolases and construction of an engineered *Pseudomonas putida* KT2440 strain

Chengyue Huang[1], Kexin Lu[1], Chenhang Ye[1], Wanyu Hu[1], Renjie Luo[1], Xuhui Zuo[1], Jun Liu[1], Maolong Zhu[1], Yuxin Yang[1], Yi Liu[1], Hanzhang Song[1], Xi Chen[2*] & Xin Yan[3*]

Abstract

Poly (butylene adipate-co-terephthalate) (PBAT), a polyester made of terephthalic acid (TPA), 1,4-butanediol and adipic acid, is extensively utilized in agricultural plastic films. However, research on the biodegradation mechanism and technological development of PBAT plastic films is still insufficient, which seriously limits its market application and leads to more serious cumulative pollution problems. This study employed error-prone PCR and site-directed mutagenesis techniques to perform directed evolution of *Ideonella sakaiensis* PETase (*Is*PETase), *Bacillus subtilis* Lipase A (*Bs*LipA) and Lipase1028, in order to achieve efficient degradation of PBAT. Furthermore, the evolved enzymes were transformed into the *Pseudomonas putida* KT2440-*tph*, constructing a KT2440 strain with high PBAT degradation capacity and the ability to utilize the terephthalic acid (TPA) and 1,4-butanediol (BDO) as carbon sources. This work offers an attractive approach for the controllable degradation of biodegradable plastics that benefits environmental sustainability.

Key words

PBAT, hydrolysis zones, KT2440, adaptive laboratory evolution; directed evolution

Introduction

Poly (butylene adipate-co-terephthalate) (PBAT), a polymer synthesized from the monomers terephthalic acid (TPA), adipic acid (AA), and 1,4-butanediol (BDO), has garnered significant attention as a biocompatible and degradable polymeric material, exhibiting considerable potential for widespread application in the realm of agricultural film technology[1-3]. However, the consequences of the growing and hard-to-reverse issue of polyethylene films on our planet are challenging, affecting both the physical environment and living organisms[4-8].

As an eco-friendly and sustainable strategy to reduce and recycle plastic waste, biodegradable catalysts using enzymes or microorganisms meet some challenges.

Firstly, the degradation of PBAT yields a mixture of TPA and AA with distinct physical and chemical properties (Figure 1). Microorganisms typically encounter carbon catabolite repression when confronted with this varied substrate mix, impeding their ability to utilize multiple substrates simultaneously. Additionally, PBAT hydrolysis products can be toxic, adversely affecting microbial metabolism and efficient substrate assimilation, particularly at high concentrations or with crude hydrolysates[9-11].

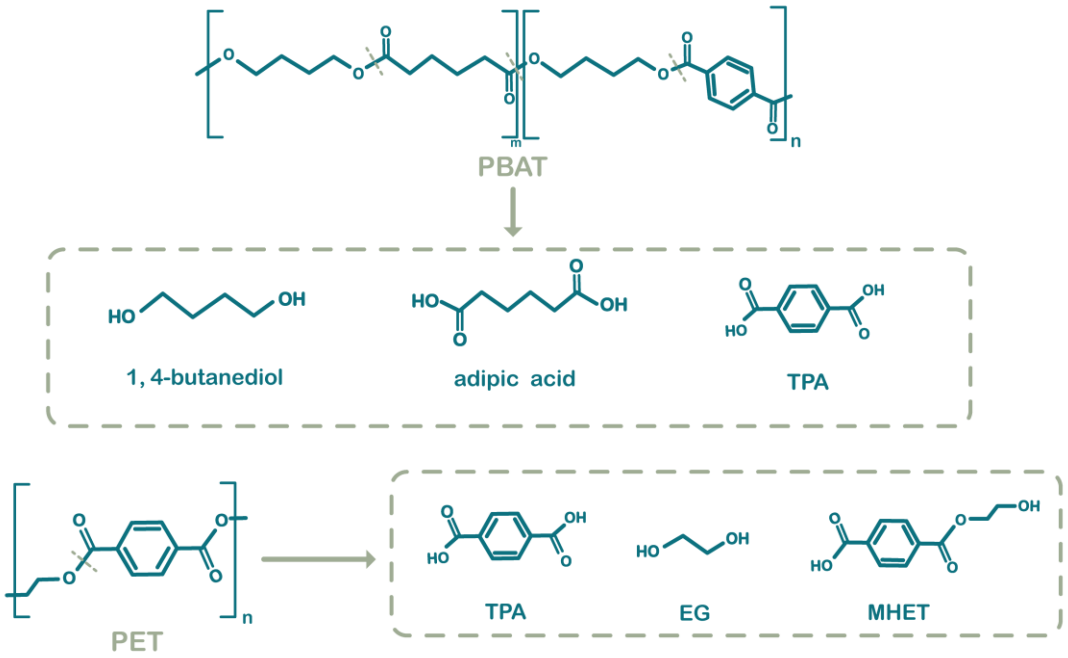

Figure 1. Chemical structures of PBAT and PET and respective ester hydrolysis products. The hydrolysis products of PBAT contain terephthalic acid (TPA), adipic acid (AA) and 1,4-butanediol (BDO) [3]. Biodegradation of PET also produces TPA, suggesting that certain enzymes that degrade PET have the potential to degrade PBAT.

Table 1. Enzymes with PBAT degradation developed in recent years

Enzyme	Classification	Source	Activity (mol/mol)*	PBAT	Condition	*Ref.*	Genbank
*Pf*L1	Lipase	*Pelosinus Fermentans*	~130	Film Milled	50℃ 72h	[12]	EIW29778.1
*Pp*Est	Esterase	*Pseudomonas Pseudoalcaligenes*	~8 ~70	Film Milled	65℃ 72h	[13]	W6R2Y2
Cbotu_EstA	Esterase	*Clostridium Botulinum*	<30	Not specified	50℃ 72h	[13]	CAL82416.1
Cbotu_EstB	Esterase	*Clostridium botulinum*	~12	Not specified	37℃ 72h	[13]	CAL83600.1
*Tf*Cut	Cutinase	*Thermobifida fusca*	5198	Film	70℃ 48h	[3]	CBY05530
*Is*PETase	Cutinase	*Ideonella sakaiensis*	4868	Film	30℃ 48h	[3]	A0A0K8P6T7
*Pb*PL	Cutinase	*Polyangium brachysporum*	-	Film	30℃ 48h	-	-
BurPL	Cutinase	*Burkholderiales bacterium*	3208	Film	35℃ 48h	[3]	-
Ple628	Hydrolases	Marine microbial consortium	121	Film	30℃ 144 h	[14]	OK558824
Ple629	Hydrolases	Marine microbial consortium	1704	Film	30℃ 72 h	[14]	OK558825
HiC	Cutinase	*Humicola insolens*	~10,000	Film	50℃ 72 h	[13]	A0A075B5G4
LCC	Cutinase	Leaf-branch compost	4636	Film	70℃ 24 h	[3]	G9BY57.1
ICCG	Cutinase	Leaf-branch compost	5275	Film	75℃ 24 h	[3]	USU85609.1
*Tc*Cut	Cutinase	*Thermobifida1 cellulosilytica*	5361	Film	65℃ 48h	[3]	ADV92526.1

*The activity is the quantitation of products containing TPA and BTa (mol) per mol enzymes.

- refers to not find.

Existing PBAT-degrading enzymes and microorganisms typically require high temperatures (50-65℃) for effective composting (Table 1) [15]. *Jia et al.* identified a serine hydrolase enzyme from *Thermobifida fusca* FXJ-1 capable of degrading PBAT at 55℃, while *Wallace et al.* utilized proteomics to isolate an esterase from *Pseudomonas pseudoalcaligenes* effective at 65℃[16]. Nevertheless, the PBAT decomposition rates of existing PBAT-degrading enzymes in room temperature are generally low, restricting its utilization in the context of agricultural practices[17]. *Wang et al.* reported that the degradation rate of PBAT films in conventional agricultural soil was only 2.3% over a three-month period[18].

In this work, we identified three distinct enzyme candidates for targeted evolutionary engineering, with the objective of developing highly efficient PBAT-degrading enzymes that exhibit optimal catalytic activity under room temperature conditions. These enzyme candidates include *Is*PETase, a cutinase derived from the PET-degrading bacterium *Ideonella sakaiensis*; *Bs*LipA, a lipase from *Bacillus subtilis*; and Lipase1028, which has been newly isolated in our laboratory. *Is*PETase is capable of degrading PET in the glassy state at moderate temperatures (30-37℃) [19-22]. *Bs*LipA exhibits good hydrolytic activity on ester bonds formed by medium-chain fatty acids[23, 24]. Lipase1028 demonstrates significant degradation capabilities for polyurethanes (PU). Based on the structural similarities between the substrates of these three enzymes and PBAT, we propose that all three possess considerable evolutionary potential[3, 25].

Furthermore, we also aim to obtain an engineering single strain capable of catabolizing of PBAT-derived degradation products. *Pseudomonas putida* has been recognized as a potential host organism for a diverse range of biotechnological applications, including the metabolic processing of plastics [26, 27]. *Wing-Jin Li et al.* reported that the wild-type *Pseudomonas putida* KT2440 could degrade TPA but at a very slow rate, requiring over 50 hours to degrade 20 mM substrate[28]. In this study, we transformed the gene cluster *tph* derived from *Pseudomonas stutzeri* TPA3 into KT2440 to enable its degradation of TPA[29, 30]. Then, we performed adaptive laboratory evolution and metabolic engineering to isolate KT2440 variants capable of utilizing 1, 4-butanediol as the sole carbon source. Ultimately, we will transform the PBAT degradation enzyme genes which are obtained from directed evolution, into the engineered KT2440 strain, aiming to create a single strain capable of efficiently degrading PBAT and utilizing its degradation products, thus facilitating sustainable degradation processes eventually.

Result

Construction and validation of the secretion pathway in *Bacillus subtilis*

We first established an efficient secretion system within *Bacillus subtilis*. The signal peptide AprE was fused to the N-terminus of the enzymes to enable them to be

effectively secreted out of the cells via the Sec pathway. In *Bacillus subtilis*, chaperones help the signal peptide to fold initially, and then SRP (signal recognition particle) combines with the signal peptide to form a complex. Chaperones, FtsY, and SecA together lead the enzyme to the Sec transport proteins. After the precursor protein traversing the membrane, the signal peptide is cleaved and degraded, and the extracellular chaperones assist the protein to form a stable conformation (Figure 2a) [31, 32]. Then we performed Prolonged Overlap Extension PCR (POE-PCR) to separately polymerize the sequences of the three enzymes and the linearized pHCM12M (Figure S1) vector into polymers (Figure 2b and S5) [33], which were then transformed into *Bacillus subtilis*.

To verify whether the enzymes were secreted out of the cells, we cultivated the bacterium on the plates with polycaprolactone (PCL), which can be hydrolyzed by lipases, esterases, keratinases and so on, commonly serving as a model substrate for assessing the extracellular secretion of hydrolases[34]. After incubating at 30 ℃ for 24 hours, all colonies exhibited distinct hydrolysis zones (Figure 2c), indicating that this pathway enables *Bacillus subtilis* a stable extracellular protein secretion capability. The successfully constructed protein exocytosis pathway allows for intuitive hydrolysis zones screening of the PBAT-degrading enzyme libraries.

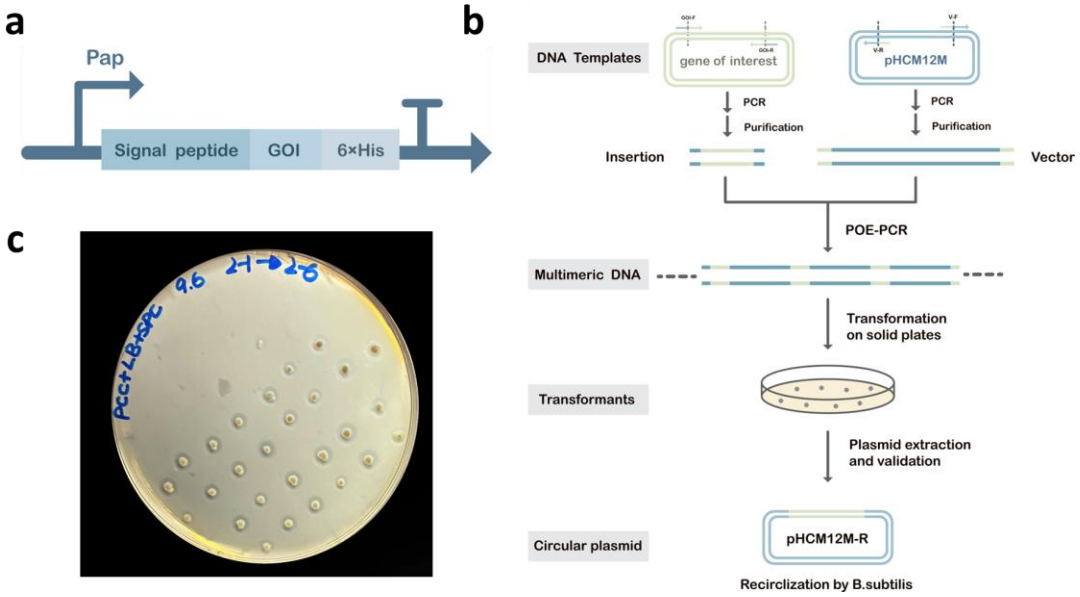

Figure 2. (a) An efficient secretion pathway in *Bacillus subtilis*. In the pathway there is the Sec signal peptide AprE separately with the genes of interest (GOI) requiring secretion downstream of it. GOI include *Is*PETase, *Bs*LipA, and Lipase1028. Downstream of the GOI is the 6×His tag for the purification of the protein; **(b) Flowchart of the prolonged overlap extension PCR (POE-PCR) process for the transformation of GOI into *Bacillus subtilis* SCK6.** We obtain the linearized vector and DNA fragment with homologous arms by PCR reaction. During POE-PCR, GOI and the vector fragments are used simultaneously as primers and templates to obtain linear multimeric DNA, which is transformed into the super competent *Bacillus subtilis* SCK6 and circularized later to form recombinant plasmids. Compared to plasmid, multimeric DNA exhibits higher transformation efficiency when transformed into *Bacillus subtilis* [33]; **(c) PCL plates**

to verify the secretion ability of *Bacillus subtilis*. *Bacillus subtilis* with recombinant plasmids were cultured on LB agar medium supplemented with PCL within 12-24 hours[34].

Construction and screening mutation libraries separately of *Is*PETase, *Bs*LipA and Lipase1028

Error-prone PCR (epPCR) and site-directed mutagenesis techniques were used to construct the mutation libraries of the 3 candidate genes, followed by a production of the variants in *B. subtilis* and screening variants by selection of phenotypes. The ratio of the diameter of the hydrolysis zone to the colony diameter can roughly reflect the ability of the variants to degrade PBAT. Firstly, the strains with successful transformants were sorted from the LB plate only with antibiotics. Then active colonies with larger hydrolysis zones were chosen from LB-agar plates supplemented 2% PBAT, followed with the next round screening to evaluate the stability and the diameter of potential colonies which were selected for further analysis (Figure 3).

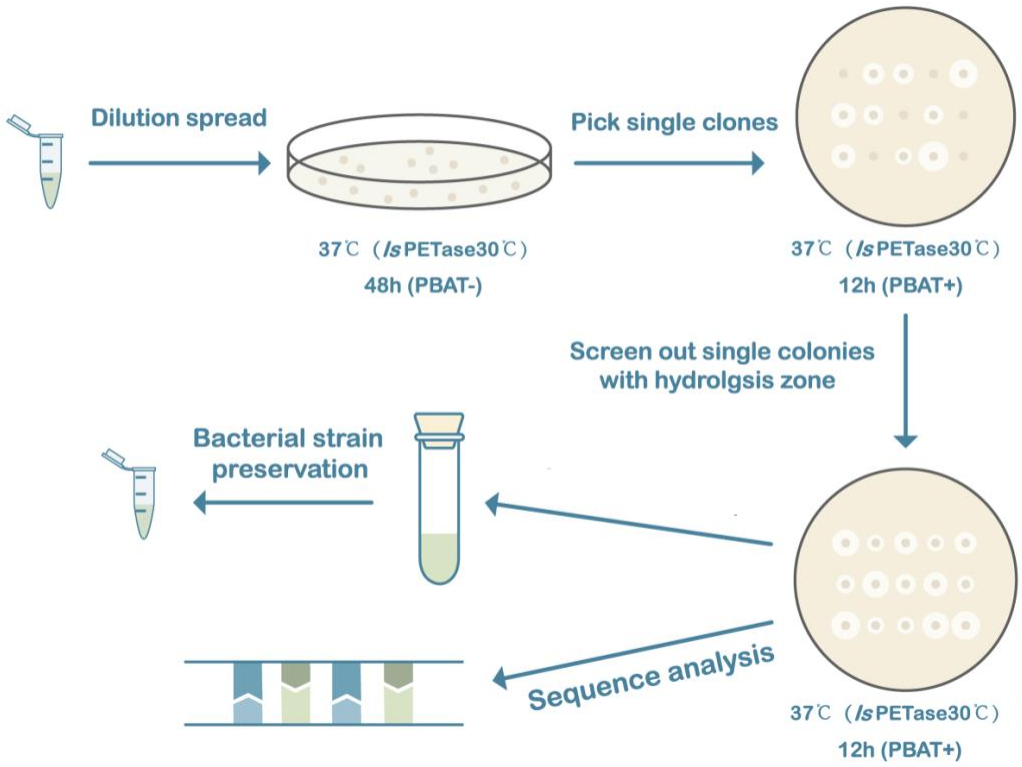

Figure 3. Screening strategies for mutation libraries.

For *Is*PETase, following two rounds of error-prone PCR, 54 plates were screened to construct a mutation library containing approximately 1,260 variants (Figure S4). In preliminary experiments, we adjust the ion environment of the PCR system through gradient experiments (Table S3). A number of strains capable of producing small hydrolysis zones were sorted, but they only possessed limited transformation efficiency,

poor growth ability and almost no mutations. These may be attributed to adaptive laboratory evolution (ALE) of the strains during growth on PBAT-containing plates, rather than mutations (Figure 4a).

Therefore, the error-prone PCR system was optimized by adjusting the concentrations of Mn^{2+} and Mg^{2+} to construct a new mutation library (Table S4), where we successfully obtained ND (New Degradable Enzyme), a variant with enhanced PBAT degradation ability. ND produced distinct hydrolysis zones after being incubated at 30℃ for 36 hours and at 37°C for 48 hours.

For the *Bs*LipA enzyme, a mutation library comprising approximately 1,220 variants was constructed through a single round of error-prone PCR. Two mutants were isolated and designated BM5 and BM10. However, when culturing these mutants on LB agar medium supplemented with PBAT, the hydrolysis zones produced by BM5 and BM10 were smaller compared to the wild type (Figure 4b).

Recently, our laboratory identified a new lipase 1028, which exhibits strong degradation ability toward polyurethane (PU). Given that both PBAT and PU are polyester-based degradable materials, we hypothesized that 1028 had evolutionary potential[35]. To test this, a mutation library comprising over 6,000 variants was constructed across 40 plates through a single round of error-prone PCR, and successfully isolated six highly efficient mutants, designated 1028_M2 through 1028_M7 (Figure 4c). These mutants exhibited clear hydrolysis zones after just 4 hours of incubation at 37℃, significantly outperforming the wild-type enzyme in PBAT degradation.

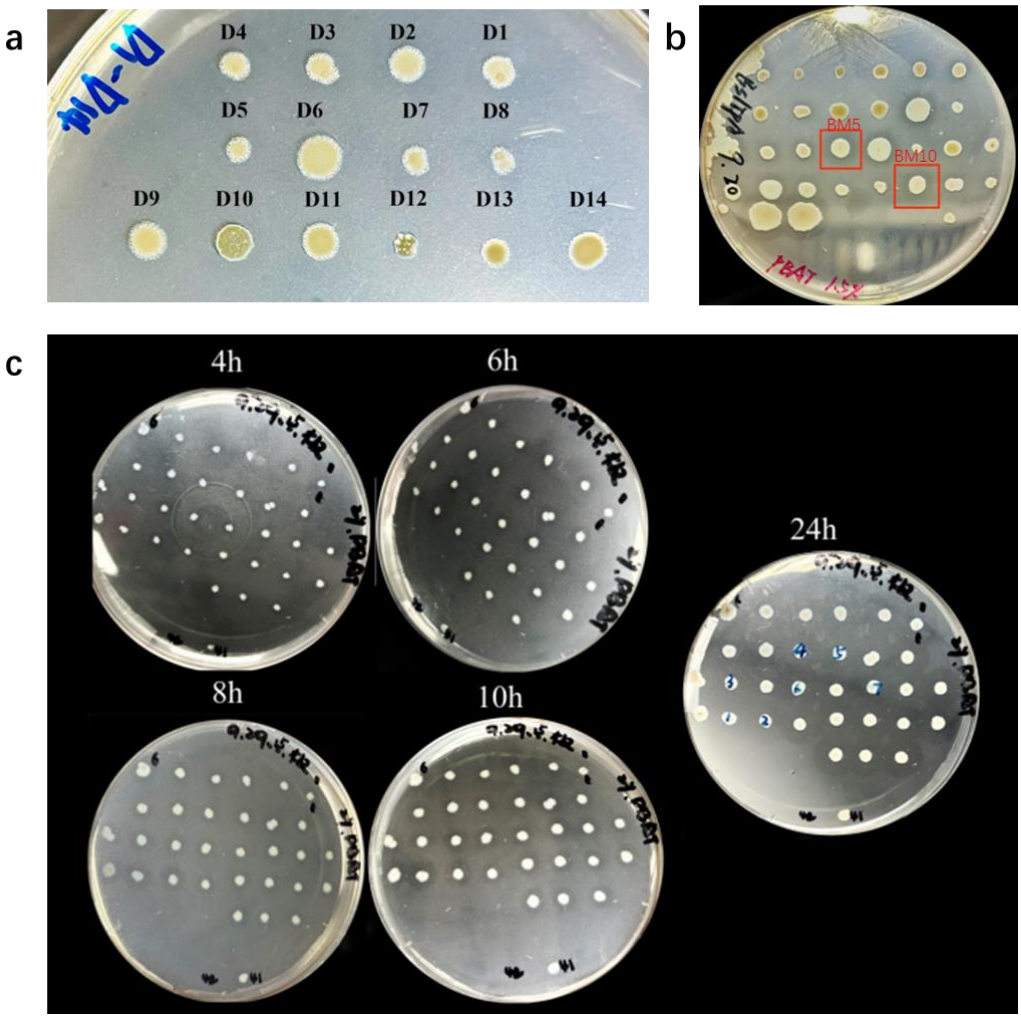

Figure 4. (a) Hydrolysis zones of *Is*PETase mutants (D1-D14). Possibly due to the lower evolutionary starting point of *Is*PET*ase*, the smaller hydrolysis zones and the generally lower degree of transparency. **(b) Hydrolysis zones of *Bs*LipA mutants.** We screened two individuals that were better on PBAT LB plates based on the ratio of the hydrolysis zones to the diameter of the bacteriophage zones and named them BM5,BM10, respectively. **(c) Hydrolysis zones of Lipase 1028 mutants.** The size of the hydrolysis zones incubated at 37℃ for 4 h, 6 h, 8 h, 10 h, and 24 h, respectively, reflected the generally higher PBAT catabolic capacity of mutants of lipase 1028.

In addition to the error-prone PCR with random mutagenesis, we performed targeted mutagenesis of three wild-type PBAT-degrading enzymes in parallel using computer simulation in order to achieve better mutation effect.

Using the web server of HotSpot Wizard 3, we scanned the highly variable residues in the catalytic pocket of *Is*PETase, resulting in the mutations of T61N, T61K, and A170S (Table 2) [36]. Then we constructed five mutant groups: A170S, T61K, T61N, T61N+A170S, and T61K+A170S. These mutants were transformed into *Bacillus subtilis* SCK6 for subsequent hydrolysis zone screening and validation. However, no

mutants with significant hydrolysis zones were obtained.

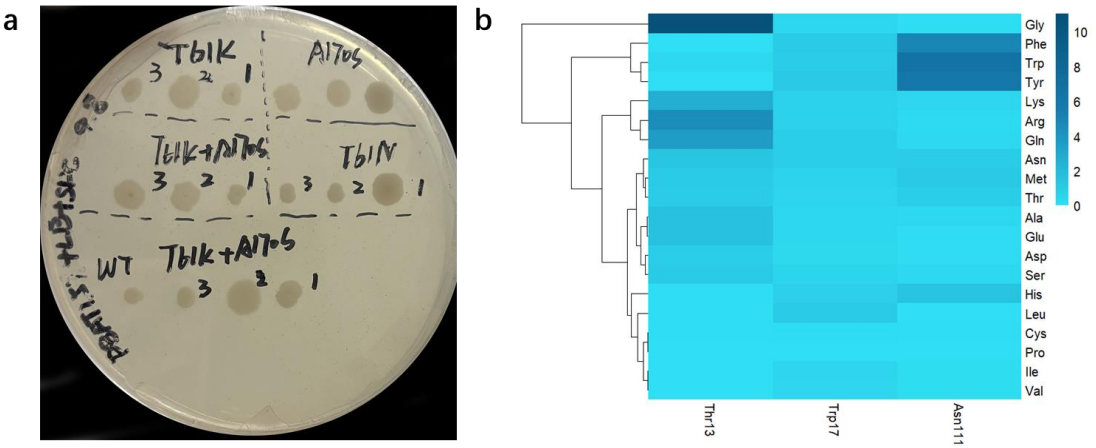

Figure 5. (a) Growth of colonies with the Site-directed mutation of *Is*PETase. No obvious hydrolysis zones were found. **(b) The amino acid mutation heatmap of the Lipase 1028.**

Table 2. Main characteristics of *Is*PETase single mutation prediction

Index	Mutation	Mutation Energy (kcal/mol)	Effect
1	A: Thr61>Asn	-0.6	STABILIZING
2	A: Thr61>Lys	-0.4	STABILIZING
3	A: Ala62>Ser	-0.4	STABILIZING

Using the same methodology, predictions for the enzyme *Bs*LipA yielded the mutation results Y75F, A75S, T101S, T111A, and A13G (Table 3). We created fifteen mutant groups: Y75F, A75S, T101S, T111A, A13G, Y75F+A75S, Y75F+T101S, Y75F+T111A, Y75F+A13G, A75S+T101S, A75S+T111A, A75S+A13G, T101S+T111A, T101S+A13G, and T111A+A13G. After computer simulation of site-directed mutations, the resulting mutation effects were all neutral mutations, so no further experimental validation was carried out, which may have some relation to our inability to obtain favorable mutations during error-prone PCR.

Table 3. Main characteristics of *Bs*LipA single mutation prediction

Index	Mutation	Mutation Energy (kcal/mol)	Effect
1	A: Tyr125>Phe	0.8	NEUTRAL
2	A: Ala75>Ser	0.9	NEUTRAL
3	A: Thr101>Ser	1.2	NEUTRAL
4	A: Thr101>Ala	1.6	NEUTRAL
5	A: Ala75>Gly	2.8	NEUTRAL

Using the same methodology, predictions for the enzyme 1028 yielded the mutation results T13G, N111W, N111Y, N111F, and T13R (Table 4). We created fifteen mutant

groups: T13G, N111W, N111Y, N111F, T13R, T13G+N111W, T13G+N111Y, T13G+N111F, T13G+T13R, N111W+N111Y,N111W+N111F,N111W+T13R, N111Y+N111F, N111Y+T13R, and N111F+T13R. We have found the above favorable sites and designed primers, but due to time limited, we have not yet performed experimental validation.

Table 4. Main characteristics of 1028 single mutation prediction

Index	Mutation	Mutation Energy (kcal/mol)	Effect
1	A: Thr13>Gly	-2.4	STABILIZING
2	A: Asn111>Trp	-1.9	STABILIZING
3	A: Asn111>Tyr	-1.8	STABILIZING
4	A: Asn111>Phe	-1.6	STABILIZING
5	A: Thr13>Arg	-1.5	STABILIZING

Morphological changes of PBAT films after degradation

To quantify the degradation ability of *Bs*LipA variants BM5 and BM10, we conducted a PBAT film degradation experiment in LB. In the experiment, the PBAT film in the blank group, which was not inoculated with any strain, remained intact without significant changes after 3 days of incubation. However, the degradation rate of *Bs*LipA film in CK gradually increased over time, exhibiting degradation characteristics such as color whitening and reduced ductility. It is worth noting that our variants BM5 and BM10 also did not demonstrate significant degradation ability on PBAT. Although they showed some degradation ability during plate screening, the treated films only had minor surface changes, and their overall morphology remained relatively stable without obvious degradation observed.

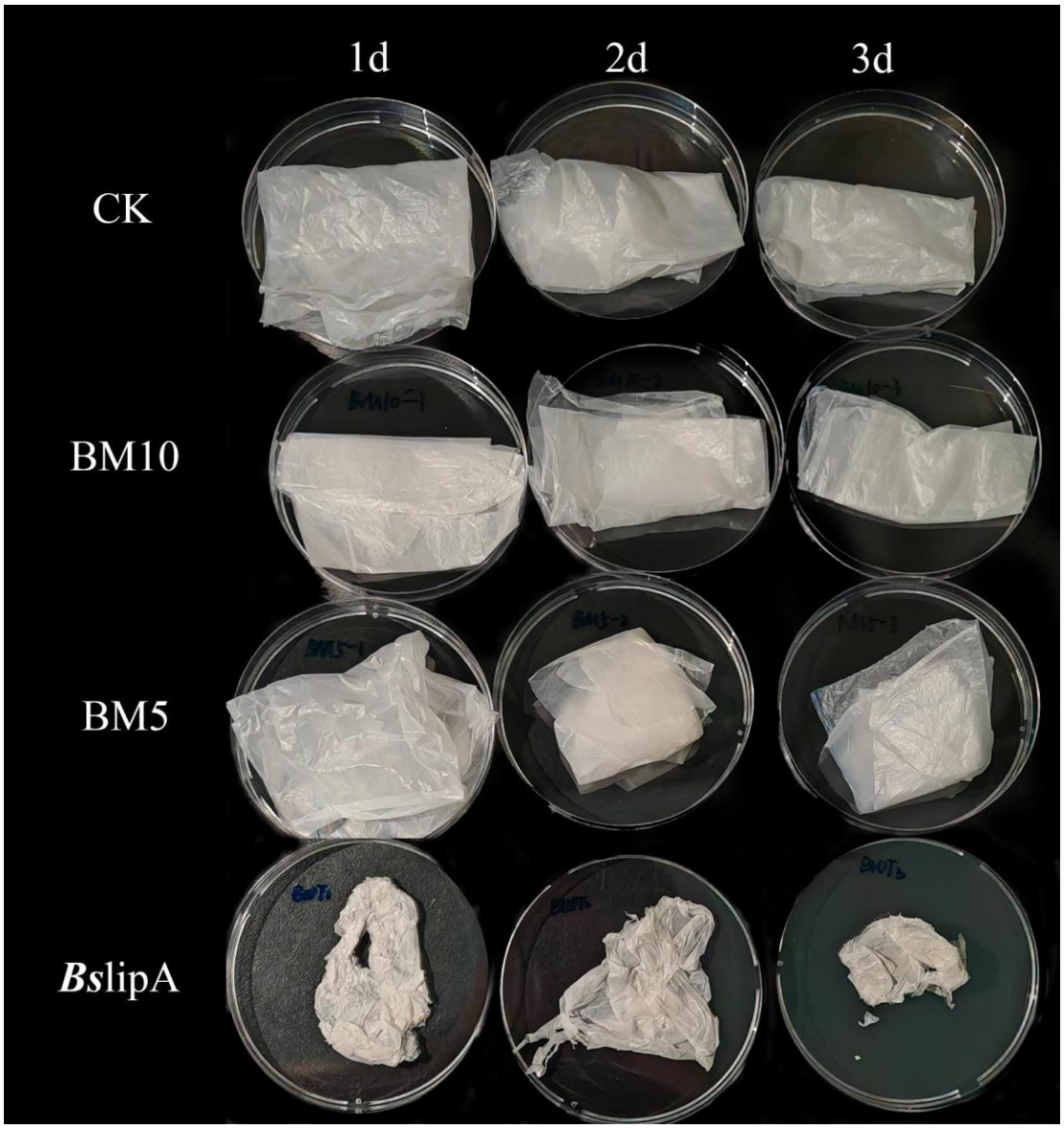

Figure 6. Morphological changes of PBAT films over different degradation periods. After incubating for 3 days in LB liquid medium without inoculated bacteria, the control group's PBAT remained intact, showing no significant changes. In the *Bs*LipA group, PBAT films exhibited increasing degradation rates, turning whiter in color and decreasing in ductility when co-incubated with different strains. Films treated with BM5 and BM10 showed relatively minor changes, with a slight reduction in overall film area and a few holes appearing on the surface.

Pathway design of a FADS-based ultra-high-throughput evolution of PBAT-degrading enzyme

The method of screening by observing hydrolysis zones is common, straightforward, cost-effective, and simple to implement. However, its efficiency is limited a lot because of following drawbacks: (1) its throughput is low (~10^4) [37]; (2) human bias when selecting colonies may happen; (3) the measurement of hydrolysis

zone size may lead to errors that affect the accuracy of the screening process; (4) the hydrolysis zones may overlap, making it challenging to accurately measure the size of each colony. Therefore, a high-throughput and precise screening method for PBAT-degrading enzymes in *B.subtilis* is needed.

A biosensor system for sensing TPA has been developed[38] (Figure 6). In this system, carboxylic acid reductase (CAR_{Mm}) from *Mycobacterium marinum* and the luciferase LuxAB from *Photorhabdus luminescens* have been transformed into *Bacillus subtilis*. TPA can enter the cells and be reduced to aldehyde by CAR_{Mm}. Then, LuxAB utilizes the aldehyde as a substrate to produce the corresponding acid, generating bioluminescence. By measuring the bioluminescence intensity at 482 nm, semi-quantitative detection of TPA can be achieved[38]. Our goal is to combine this system with FADS, which couples the activity of each mutants with the fluorescence intensity, and finally facilitates high-throughput screening (~10^7) [37, 39].

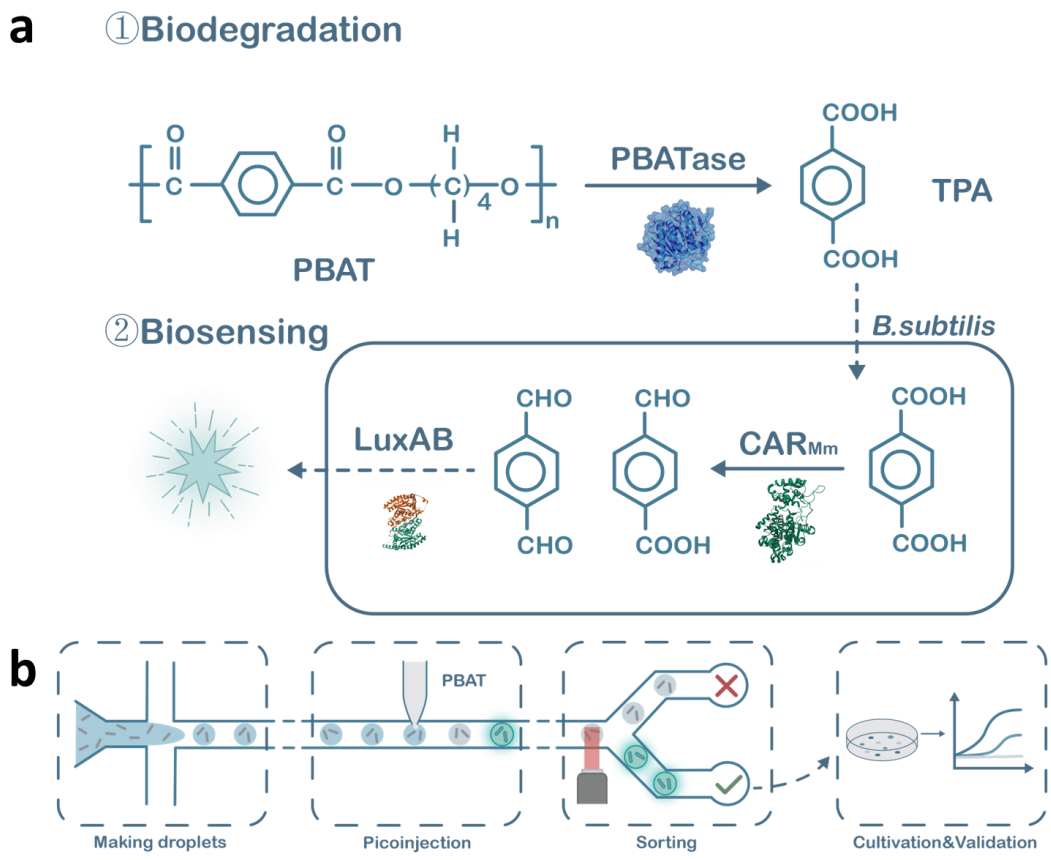

Figure 7. Biosensor-based TPA detection coupled with bioluminescent FADS screening. (a) An enzyme-coupled biosensor for detecting TPA produced by PBAT degradation. (1) PBAT enzymes degrade PBAT, releasing monomer molecules including TPA, BDO, and AA. The structure of the PBAT hydrolase is derived from our evolutionarily screened ND. (BDO and AA are not shown). (2) TPA can be reduced by CAR_{Mm} to the corresponding dialdehyde and monoaldehyde (ligand molecule PPTNi not shown). These aldehydes serve as substrates for LuxAB to generate corresponding acids and emit fluorescence, achieving bioluminescence. The excitation wavelength of the LuxAB reaction is 482 nm, which belongs to the visible cyan light spectrum. **(b) Schematic**

diagram of FADS screening process. *Bacillus subtilis* is encapsulated in microfluidic droplets and incubated to allow cells to fully express PBAT hydrolase, CAR_{Mm}, and LuxAB. After a period of incubation, PBAT is injected into the microfluidic droplets to generate a fluorescent signal. Fluorescence signal detection and sorting are then performed to separate target droplets from non-target droplets. Droplets with strong fluorescence signals typically contain the target enzymes or cells with specific biochemical reaction products, while droplets with weaker fluorescence signals are considered non-target droplets. A highly active PBAT enzyme can degrade more TPA and achieve a higher level of luminescence.

Construction of engineered KT2440 strain

To achieve the effective solution for upcycling of PBAT, a multifunctional host *P. putida* KT2440 that can secrete PET hydrolase and at the same time, completely degrade the PBAT hydrolysate TPA and BDO (Figure 8a). In the future work, we will convert the PBAT hydrolase into engineered *P. putida* KT2440-*tph* so that it can degrade PBAT and then use the degradation products for growth to achieve sustainable degradation (Figure 8b).

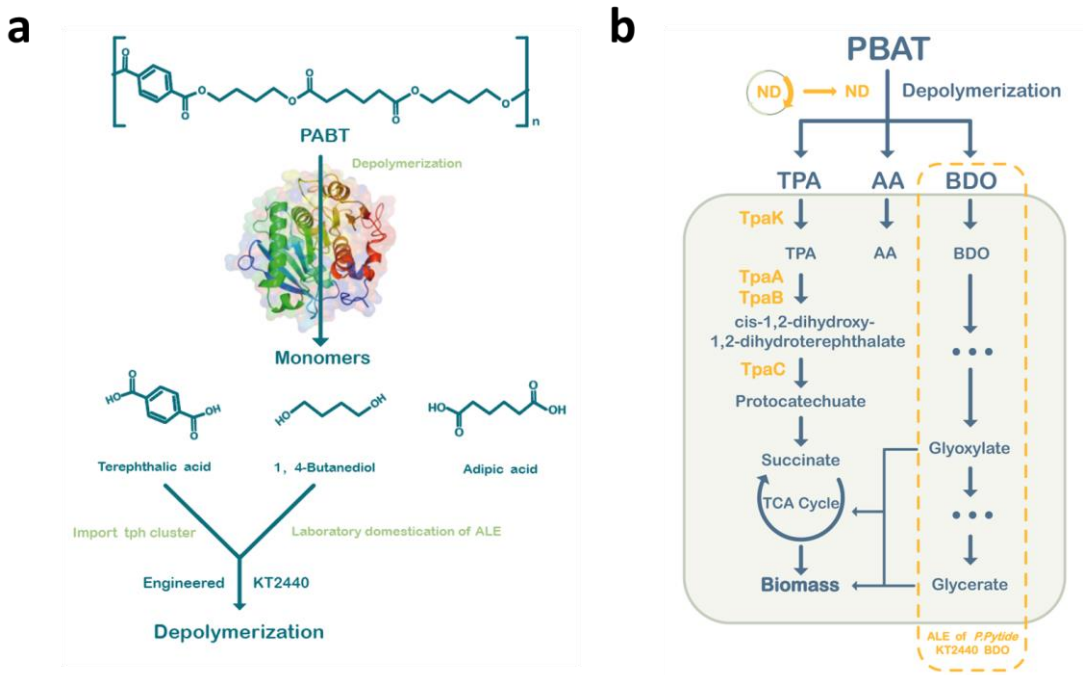

Figure 8. (a) The construction process for engineered KT2440. The engineering modification of *Pseudomonas putida* KT2440 mainly consists of three parts: (1) transforming the *tph* gene cluster into KT2440 to obtain KT2440-*tph* and expressing the gene cluster constitutively; (2) adaptive laboratory evolution (ALE) of KT2440-*tph* to enable the utilization of TPA as carbon sources and a certain concentration of 1,4-butanediol; (3) transforming the mutants into the evolved KT2440-*tph*. **(b) An engineered *P. putida* strain with abilities of PBAT depolymerization and co-degradation of TPA and BDO.** Schematic of a single engineered strain *Pseudomonas putida* KT2440 capable

of degrading PBAT and co-degrading its degradation products TPA and BDO. The entire *tph* gene cluster was transformed into KT2440 and constitutively expressed to achieve co-degradation of TPA and BDO.

It is reported that microorganisms capable of utilizing TPA include *Comamonas*, *Rhodococcus*, and *Pseudomonas* in the natural environment[40-42]. We transformed the *tph* gene cluster (Figure 9) from *Pseudomonas stutzeri* TPA3 into KT2440 via electroporation to obtain the KT2440-*tph* strain, thereby enabling the degradation of terephthalic acid (TPA) [43]. The wild-type KT2440 inherently possesses chloramphenicol resistance, while the *tph* gene cluster plasmid contains kanamycin resistance. We successfully screened for the KT2440-*tph* strain harboring the *tph* cluster on LB agar medium supplemented with chloramphenicol and kanamycin.

Figure 9. The feature of *tph* cluster. A *tph* cluster containing genes encoding the transcriptional regulator (*tphR*), tpa transporter (*tpaK*), tpa 1, 2-dioxygenase (*tphA*), and 1, 2-dihydroxy-3, 5-cyclohexadiene-1, 4-dicarboxylate dehydrogenase (*tphB*).

Isolation of KT2440-*tph* mutants capable of utilizing 1, 4-butanediol as a carbon source through adaptive laboratory evolution

Given the fact that *P.putida* KT2440 possesses the genetic inventory allowing growth on 1,4-butanediol as C-source [44], we speculated that ALE might select for 1,4-butanediol utilizing mutants. Therefore, we performed two independent ALE experiments, wild-type strain of *P.putida* KT2440 and KT2440-*tph* respectively, and different mineral salt medium (MSM) supplemented with 1,4-butanediol and TPA as sole carbon source: measure the optical density at 600 nm (OD_{600}) every 12 hours, and re-inoculated the strains once they reached the stationary phase with a total of three rounds of subculturing (Figure 10). The results indicated that as the iterative cultivation progressed, the growth rate of both the wild-type KT2440 and KT2440-tph continuously increased, demonstrating a stronger capability to utilize BDO and TPA. We plan to continue ALE in subsequent experiments to enhance their ability of degrading BDO and TPA, aiming to achieve rapid clearance of PBAT degradation products.

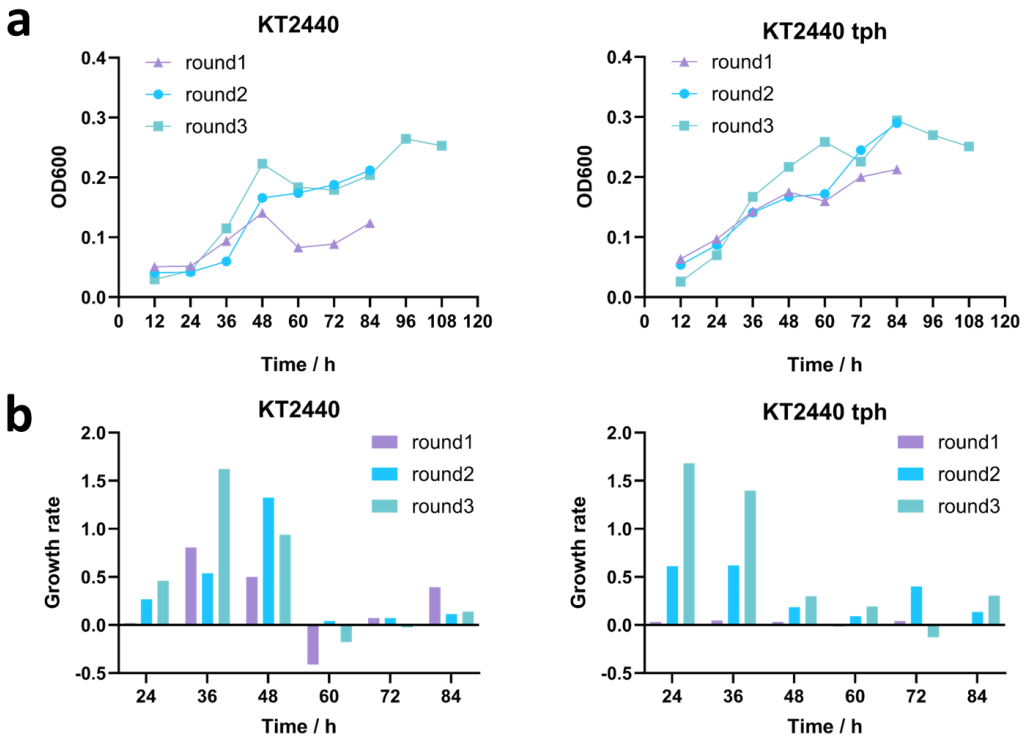

Figure 10. Adaptive laboratory evolution (ALE) growth curves (a) and growth rate curves (b) of KT2440 and KT2440-*tph*. Three consecutive rounds of cultivation were conducted, with OD600 measured every 12 hours. In the minimal salt medium for KT2440, BDO was added as the sole carbon source; for KT2440-*tph*, the medium was supplemented with TPA as the sole carbon source. The results indicated that as the iterative cultivation progressed, the growth ability of KT2440 gradually increased, which was particularly evident during the first 48 hours. (1) In terms of the maximum OD_{600} values, the third round showed the highest value, with KT2440 and KT2440-*tph* separately achieving 113.96% and 101.44% of the values observed in the second round, and 187.52% and 138.12% of the values in the first round, respectively; (2) Regarding the maximum growth rates, the third round also demonstrated a significant advantage, with KT2440 and KT2440-*tph* separately exhibiting 1.22 times and 2.71 times the growth rates of the second round, and 2 times and 36.52 times the growth rates of the first round. These suggests that both KT2440 and KT2440-*tph* have increasingly strengthened their ability to utilize BDO or TPA as the carbon source with each round of iterative cultivation.

Discussion

In this study, we provided an effective solution for the continuous valorization of PBAT. We aim to obtain an engineering multifunctional strain capable of 1, 4-butanediol and TPA as sole carbon source accompanied by the production of extracellular engineered PBAT hydrolase. This is more simplified and low-cost than the process of using recombinant *B. subtilis* to produce enzymes and then using another

strain for PBAT hydrolysate conversion. Regarding the evolution of *Is*PETase and *Bs*LipA, it is regrettable that no variants with PBAT degradation capability was selected (or the hydrolysis zones were too vague to be identified visually, leading to their neglect). Meanwhile, the performance of Lipase1028 was pleasantly surprising, and there was anticipation for the selection of mutants with strong PBAT degradation capabilities at room temperatures in subsequent work. Additionally, adaptive laboratory evolution (ALE) was conducted on the wild-type *Pseudomonas putida* KT2440 strain and the KT2440 strain harboring the *tph* cluster to enhance their ability to grow on BDO or TPA as the sole carbon sources. The results indicated that as continuous cultivation proceeds, the ability of KT2440 (or KT2440-*tph*) to utilize BDO (or TPA) have continuously improved, and it is hoped that with the progress of adaptive evolution, a chassis strain capable of efficiently clearing PBAT degradation products can be obtained.

Although the directed evolution strategy used has produced a certain number of variants around the three enzymes, the overall mutation library was small. In addition, the lack of effective screening methods was also a main obstacle. The unclear hydrolysis zones considered the biggest challenge that limits screening efficiency, as weak advantageous mutations cannot be accumulated, resulting in the inability to capture the significant performance improvement caused by the accumulation of weak advantageous mutations through multiple rounds of continuous epPCR (commonly known as low evolutionary starting point and high evolutionary difficulty). The evolutionary failure of *Is*PETase is considered a representative of this. There are two ways to try to avoid this problem: one is to reduce screening pressure and promote the accumulation of favorable mutations, and the other is to use more accurate and high-resolution screening methods to accurately identify weakly improved mutants. The former can try to adopt the concept of "evolutionary stepping stones" [45] and select appropriate PBAT mode molecules [3], namely small molecules with PBAT polymer structures that do not have the complex spatial structure of PBAT polymers, which can reduce the difficulty of substrate molecules entering the active pocket. The latter can attempt to couple the degradation degree of PBAT with fluorescence intensity, quantitatively reflecting the degradation of PBAT, as we have attempted to design a high-throughput FADS screening method based on TPA biosensing. In addition, due to the complex and stable molecular structure of polymers, limited active center structure of enzyme pockets, and lack of efficient screening methods, the evolution of polymer hydrolases often faces significant challenges. In recent years, the development of continuous directed evolution methods in vivo has provided new ideas for the evolution of polymeric hydrolytic enzymes such as *Is*PETase, and it is particularly important to seek an efficient evolutionary method for developing PBAT degrading enzymes.

Surprisingly, during our work, we sorted a strain with a strong activity of degrading PBAT (Figure S6), which was designated as ND (New Degradable Enzymes). We then conducted a series of experiments to assess its ability to degrade PBAT, and employed bioinformatics analysis, which both demonstrated its effective PBAT degradation

capacity. However, in the final analysis of its amino acid sequence, we found it is highly similar to the published PBAT degrading enzyme *Tf*Cut, which may have been used in our laboratory. Under the suspicion that ND might have been contaminated with *Tf*Cut for unknown reasons during the experimental process, we placed a large amount of related work in the supplementary materials for discussion (Figures S7, S10-S14), without including it as part of the results report. It is important to note that, because of the deadline for manuscript submission, we could not confirm whether ND is indeed *Tf*Cut; therefore, we did not completely remove the relevant content.

Finally, we hope that the successful construction of engineered KT2440 for complete degradation of PBAT will guide the construction of engineered Bacillus subtilis for complete degradation of PBAT in the future. By evolving its heat resistance, we aim to obtain spores that can withstand high temperature processes in PBAT membrane production, thereby producing PBAT "live plastics" containing modified Bacillus subtilis and achieving automated and complete biodegradation of PBAT[46]. In summary, this work has profound significance for environmental protection. The technology of efficiently degrading PBAT at room temperature can effectively reduce the residual amount of PBAT film in farmland, reduce the risk of microplastic formation, protect soil structure and ecosystem health, alleviate the problem of "white pollution", reduce the recycling cost of PBAT film, increase agricultural economic benefits, and promote food security and sustainable agricultural development.

Materials and Methods

1. Chemicals and Strain cultivation

PBAT (Provided by Yan Xin Lab, Nanjing Agricultural University); Yeast Extract (OXOID, cat. no. LP0021): TRYPTONE (OXOID, cat. no. LP0042); Agar (Solarbio, cat. no. A8190); Kanamycin (Solarbio, cat. no. K8020); Spectinomycin (Solarbio, cat. no. IS3340); Chloramphenicol (Solarbio, cat. no. C8050); 1,4-Butanediol (MACKLIN, cat. no. B802727); TPA (MACKLIN, cat. no. T880015); Magnesium Chloride (Solarbio, cat. no. M8161); Manganese Chloride (Solarbio, cat. no. M88800); NaCl (HUSHI, cat. no. 10019318); LB Liquid Medium (Add yeast extract, tryptone, NaCl to a final concentration of 5 g/L, 10 g/L, 10 g/L in water, respectively); LB Solid Medium (Add yeast extract, tryptone, NaCl, agar to a final concentration of 5 g/L, 10 g/L, 10 g/L, 1.5% agar in water, respectively); LB Solid Medium with 0.5% PBAT (Add yeast extract, tryptone, NaCl, agar to a final concentration of 5 g/L, 10 g/L, 10 g/L, 1.5% agar, 0.5% PBAT mother liquid SPC 100 mg/ml in water, respectively); LB Solid Medium with 1% PBAT (Add yeast extract, tryptone, NaCl, agar to a final concentration of 5 g/L, 10 g/L, 10 g/L, 1.5% agar, 1% PBAT mother liquid SPC 100 mg/ml in water, respectively); LB Solid Medium with 1.5% PBAT (Add yeast extract, tryptone, NaCl, agar to a final concentration of 5 g/L, 10 g/L, 10 g/L, 1.5% agar, 1.5% PBAT mother liquid SPC 100 mg/ml in water, respectively); SPC Resistance Screening Medium (Add

yeast extract, tryptone, NaCl, agar to a final concentration of 5 g/L, 10 g/L, 10 g/L, 1.5% agar, SPC 100 mg/ml in water, respectively); Chl SPC Resistance Screening Medium (Add yeast extract, tryptone, NaCl, agar to a final concentration of 5 g/L, 10 g/L, 10 g/L, 1.5% agar, SPC 100 mg/ml, Chl 30 mg/ml in water, respectively).

2. Plasmids and Strains

The lipase used in the experiment comes from the strain YX8[47], and the PETase enzyme, PHCM12M, KT2440, lipase1028, as well as the positive control, are all provided by Professor YanXin's laboratory at Nanjing Agricultural University. The pBBR1MCS-2-*tph* was kindly gifted by Professor Su Tianyuan from Shandong University.

3. Preparation of PBAT Stock Solution

Weigh 0.5 grams of PBAT granules and add them to a centrifuge tube along with 20 mL of hexafluoroisopropanol to create a solution. In a conical flask, add 100 mL of ddH2O and maintain the water temperature at around 60°C. Once the materials in the centrifuge tube are completely dissolved, slowly add the solution to the water in the conical flask while continuously shaking to prevent clumping. After adding the PBAT solution, place the conical flask in a 60°C shaking water bath for three days, and during this process, be sure to prevent the water from evaporating by regularly adding water to the water bath as needed.

4. Monitoring degradation ability of different enzymes for PBAT-based films

To determine the degradation capacity of different enzymes on PBAT, single colonies of bacteria containing various enzymes are picked and transferred into 100 ml of LB medium containing 100SPC (100 mg/ml). Then, a piece of sterile pure PBAT film (15 cm × 15 cm) is added to the culture medium. The cultures are incubated at 37°C with shaking at 180 rpm, with *Is*PETase being incubated at 30°C. Photographs are taken every 24 hours for a period of 5 days to record the degradation process.

5. Morphological observation of the films

Overall changes in the films were recorded by camera. The broken film is collected by filtration through cheesecloth, air-dried, and then photographed.

6. Error-Prone PCR

6.1 Using the (StarMut) Error-Prone PCR Kit

Add 25 μL of 2 × Rapid Taq Master Mix (Green Enzyme), 1 μL each of forward and reverse primers, 10 ng of PETase or *Bs*LipA, 1-10 μL of StarMut DNA Enhancer, make

up to a final volume of 50 μL with water. The error-prone PCR program is as follows: Initial denaturation at 95°C for 2 minutes, denaturation at 94°C for 30 seconds, annealing at 56°C for 1 minute, extension at 72°C for 60 seconds per kilobase (kb) (30 cycles), final extension at 72°C for 7 minutes.

6.2 Not using the (StarMut) Error-Prone PCR Kit

Prepare six 50 μL error-prone PCR systems with varying concentrations of Mg^{2}+ and Mn^{2+}, 25 μL of 2 × Phanta Max Buffer,1μL dNTP Mix(10mM each),1 μL Phanta Max Super-Fidelity DNA Polymerase, 1 μL each of primer F and R, 1 μL of DNA Template (10 ng), 1/1/1/2/2/2 μL of $MnCl_2$ solution (25 mM), 0.5/1/2/0.5/1/2 μL of $MgCl_2$ solution (25 mM),adjust the volume with ddH_2O to 18.5/18/17/17.5/17/16 μL respectively. The PCR program is as follows: initial denaturation at 95°C for 3 minutes, denaturation at 94°C for 30 seconds, annealing at the primer's Tm for 30 seconds,extension at 72°C for 1 minute per kilobase (kb) (45 cycles), final extension at 72°C for 5 minutes.

7. POE-PCR (Prolonged overlap extension PCR)

Using the (Vazyme) Phanta Max Super-Fidelity DNA Polymerase Kit: add 25 μL of 2× Buffer,1 μL of dNTP Mix (10 mM each),1 μL of Phanta Max Super-Fidelity DNA Polymerase, the vector fragment and the target gene fragment according to the ratio of their lengths, make up to a final volume of 50 μL with ddH_2O. The PCR program is as follows: initial denaturation at 95°C for 3 minutes, denaturation at 95°C for 15 seconds, annealing at 60°C for 30 seconds, extension at 72°C for 90 seconds per kilobase (kb) (perform 30 cycles),final extension at 72°C for 12 minutes.

8. Preparation of Competent Cells SCK6

Retrieve the *Bacillus subtilis* SCK6 strain stored at -80°C and streak it on an LB agar plate to activate it. Pick a single colony from the streaked plate and inoculate it into fresh LB liquid medium. Incubate the culture overnight at 30°C with shaking at 220 rpm for 12 hours. Transfer the overnight culture into fresh LB liquid medium containing 1% xylose, starting with an OD600 of 1.0. Continue incubation at 37°C with shaking at 220 rpm for 2 hours. The resulting bacterial culture is now competent. Aliquot the competent cells. Add 10% glycerol to each aliquot. Store the aliquots at -80°C for long-term preservation.

9. Transformation Procedure

Prepare plates by pouring 80 mL of solid LB medium and adding 80 μL of antibiotic solution (100 mg/ml) to each plate. Thaw the competent cells (SCK6) on ice. Add the polymer (e.g., polyethylene glycol, PEG) to the competent cells based on the brightness of the gel after electrophoresis; typically, 3 or 5 μL is sufficient. Transfer the cells with

added polymer to an EP tube and secure the tube in a 37°C shaker incubator for one hour. Perform the plating in two steps: a. For the first plating, do not centrifuge or resuspend the cells. Directly plate 100 μL of the bacterial suspension per plate. b. For the second plating, centrifuge the remaining bacterial suspension from the first plating at 5000 rpm for 2 minutes. Discard the supernatant, retain 100 μL of the culture medium, resuspend the pellet, and plate. Incubate the plates overnight at 37°C.

This procedure allows the competent cells to take up the DNA or other genetic material contained in the polymer, leading to the transformation of the bacteria. The incubation step allows the transformed cells to grow into colonies that can be observed and selected the following day.

10. Screening mutant libraries separately of IsPETase, *Bs*LipA and Lipase1028

The qualitative method for assessing the hydrolytic ability of mutants is to observe the diameter of the transparent hydrolytic zone on the agar plate.

11. Colony PCR Procedure

First, add 27 μL of Lysis Solution I and 3 μL of Lysis Solution II, then transfer the bacterial colony. Treat at 72°C for 20 minutes. After the treatment, quickly add 3 μL of Lysis Solution III. Take 3-5 μL of the above reaction system as the template for the reaction. Add 25 μL of Green Enzyme, 2 μL of primers F/R, and make up to 50 μL with ddH2O. Proceed with the PCR reaction using the following program: initial denaturation at 95°C for 30 seconds, denaturation at 95°C for 15 seconds, annealing at 56°C for 15 seconds, extension at 72°C for (length in kb × 30 seconds) per cycle, set for 30 cycles, final extension at 72°C for 5 minutes.

12. Preparation of KT2440 Competent Cells

Distribute the KT2440 culture into pre-sterilized 50ml centrifuge tubes and balance them. Centrifuge at 4°C, 5000rpm, for 5 minutes. After centrifugation, discard the supernatant, add 10-15ml of 15% glycerol, and mix well. After mixing, balance again, centrifuge at 4°C, 5000rpm, for 5 minutes. Repeat the above steps three times, and after the third centrifugation, discard the supernatant. Resuspend in 2ml of 15% glycerol to obtain KT2440 competent cells. Aliquot into 1.5ml EP tubes and store in a -20°C freezer. Electrotransformation Method to Transfer the *tph* Cluster into KT2440 Competent Cells. Take 90μl of competent cells in a PCR tube, add 2000ng of plasmid DNA (calculated according to the nucleic acid concentration), mix well, and let it stand in an ice box for 3 minutes. Take out the pre-chilled electroporation cuvette, transfer 100μl of the mixed solution from the PCR tube into the electroporation cuvette. Wipe the outside of the cuvette to remove any water, and perform electroporation with the following parameters: 1500V, 25μF, 200Ω, 1mm. After electroporation, add 500μl of LB broth to the cuvette, mix well to wash out all the liquid, thus obtaining the KT2440 strain containing the *tph*

cluster. Incubate at 30°C on a shaker for 3 hours. After 3 hours of incubation, take out the culture, and from one EP tube (containing 600μl), spread 100μl onto a plate containing both chloramphenicol (Chl 30μg/ml) and kanamycin (Kan 50μg/ml). Centrifuge at 5000rpm for 2 minutes. Aspirate about 400μl of the supernatant, and spread the remaining 100μl onto the plate.

13. Adaptive Laboratory Transformation of KT2440 and KT2440-tph

Prepare 5ml of LB liquid medium and add 2μl of chloramphenicol (50,000 ppm), or add 1ml of chloramphenicol and 1ml of kanamycin, respectively. Inoculate single colonies of KT2440 and KT2440-*tph* into the tubes containing the antibiotic medium. Incubate the cultures in a shaker at 30°C and 180rpm for 24-36 hours until the OD600 reaches 1.0-2.0. Transfer the cultures to 2ml centrifuge tubes under sterile conditions in a laminar flow hood. Centrifuge at 6000 rpm for 3 minutes, discard the supernatant, and resuspend the pellet in 1ml of sterile water by vortexing to ensure complete resuspension without any sediment. Centrifuge again at 6000 rpm for 3 minutes, discard the supernatant, and repeat this washing step three times. Finally, resuspend the pellet in 500μl-1ml of sterile water to make the inoculation stock. Inoculate the stock into a conical flask containing 20ml of mineral salt medium with 300ppm of 1,4-butanediol. Cultivate the culture in a shaker at 30°C, and measure the OD600 every 12 hours.

14. Molecular Docking [48]

Protein-small molecule docking was performed using AutoDock 4.2.6 []. The 3D structure of the protein receptor was obtained using AlphaFold3, and the planar conformation of BABTaB was obtained from PubChem, and then conformational conversion was performed using Rdkit to form the optimal 3D conformation required for docking and stored as a mol2 format file . Using AutoDockTools (ADT), we performed operations such as adding hydrogens to BABTaB and merging nonpolar hydrogen atoms, and calculated Gasteiger-Huiekel charges. The ligand was also stored as a file in PDBQT format.

The LGA algorithm energy optimisation was chosen and the Autogrid4 docking box and Autodock4 docking program with the relevant parameters were set to finally obtain the binding energies of the various docked conformers aggregated and the computer selected the binding energy with the lowest docking result and then used this docked conformation as a reference to compare the other docking results. The final screened conformations were analysed and plotted using Pymol.

15. Prediction of Single Mutation Sites

Use the HotSpot Wizard 3.0 web server to predict mutation sites. Utilize the functional hotspots corresponding to highly mutable residues located in the active site pocket or access tunnels module of the HotSpot Wizard 3.0 online service to predict the sites of

mutation. This is done by calculating the mutation energy protocol to assess the stability of mutations at individual sites.The mutation energy (binding) protocol evaluates the impact of single-point mutations on protein stability. It performs an amino acid scan mutagenesis on a set of selected amino acid residues, mutating each amino acid residue to one or more specific types of amino acids. Mutation energy is the change in protein stability caused by the mutation. It is xmeasured by comparing how much energy is required for the protein to fold in its original and mutated forms. The more energy a protein requires to fold, the less stable it is.

16. Molecular Dynamics (MD) Simulation

Molecular dynamics (MD) simulations are performed using GROMACS 2024.03 software. The CHARMM36 force field and CHARMM General Force Field are used to generate parameters and topological structures for proteins and ligands, respectively. Each atom of the protein is optimized with a distance greater than 1.0 nm. The protein is then solvated with water molecules at a density of 1. The simulation system is neutralized by replacing water molecules with CLA^- and SOD^+ ions. Energy minimization is performed using the steepest descent method for 5.0×10^4 steps to minimize the energy consumption of the entire system, ultimately reducing unreasonable contacts or atomic overlaps in the entire system. After energy minimization, the first phase of equilibration is carried out at 300 K for 100 ps to stabilize the system's temperature. The second phase of equilibration is simulated under NPT conditions at 1 bar for 100 ps. The main purpose of the simulation is to optimize the interactions between the target protein and solvents and ions, ensuring that the simulation system is fully pre-equilibrated. All MD simulations are carried out under isothermal and isostatic conditions at a temperature of 300 K and an atmospheric pressure of 1 bar for a duration of 50 ns.

Reference

[1] A. Kanwal, M. Zhang, F. Sharaf and C. Li, Polymer pollution and its solutions with special emphasis on Poly (butylene adipate terephthalate (PBAT)), *Polymer Bulletin*, **79**, **9303-9330,** (**2022**).
DOI: https://doi.org/10.1007/s00289-021-04065-2

[2] S. Roy and J.-W. Rhim, Curcumin Incorporated Poly(Butylene Adipate-co-Terephthalate) Film with Improved Water Vapor Barrier and Antioxidant Properties, *Materials*, **13**, (**2020**).
DOI: https://doi.org/10.3390/ma13194369

[3] Y. Yang, J. Min, T. Xue, P. Jiang, X. Liu, R. Peng, et al., Complete bio-degradation of poly(butylene adipate-co-terephthalate) via engineered cutinases, *Nature Communications*, **14**, (**2023**).
DOI: https://doi.org/10.1038/s41467-023-37374-3

[4] M. C. Rillig, Microplastic in Terrestrial Ecosystems and the Soil?, *Environmental Science & Technology*, **46**, **6453-6454,** (**2012**).
DOI: https://doi.org/10.1021/es302011r

[5] Z. Liu, F. Huang, B. Wang, Z. Li, C. Zhao, R. Ding, et al., Soil respiration in response to biotic and abiotic factors under different mulching measures on rain-fed farmland, *Soil & Tillage Research*, **232**,

(**2023**).
DOI: https://doi.org/10.1016/j.still.2023.105749
[6] Z. Steinmetz, C. Wollmann, M. Schaefer, C. Buchmann, J. David, J. Troeger, et al., Plastic mulching in agriculture. Trading short-term agronomic benefits for long-term soil degradation?, *Science of the Total Environment*, **550**, **690-705,** (**2016**).
DOI: https://doi.org/10.1016/j.scitotenv.2016.01.153
[7] R. M. Qi, D. L. Jones, Z. Li, Q. Liu and C. R. Yan, Behavior of microplastics and plastic film residues in the soil environment: A critical review, *Science of the Total Environment*, **703**, (**2020**).
DOI: https://doi.org/10.1016/j.scitotenv.2019.134722
[8] D. Brennecke, B. Duarte, F. Paiva, I. Caçador and J. Canning-Clode, Microplastics as vector for heavy metal contamination from the marine environment, *Estuarine Coastal and Shelf Science*, **178**, **189-195,** (**2016**).
DOI: https://doi.org/10.1016/j.ecss.2015.12.003
[9] M. N. Kim, B. Y. Lee, I. M. Lee, H. S. Lee and J. S. Yoon, Toxicity and biodegradation of products from polyester hydrolysis, *Journal of Environmental Science and Health Part a-Toxic/Hazardous Substances & Environmental Engineering*, **36**, **447-463,** (**2001**).
DOI: https://doi.org/10.1081/ese-100103475
[10] J. F. Pang, M. Y. Zheng, R. Y. Sun, A. Q. Wang, X. D. Wang and T. Zhang, Synthesis of ethylene glycol and terephthalic acid from biomass for producing PET, *Green Chemistry*, **18**, **342-359,** (**2016**).
DOI: https://doi.org/10.1039/c5gc01771h
[11] K. Varaprasad, M. Pariguana, G. M. Raghavendra, T. Jayaramudu and E. R. Sadiku, Development of biodegradable metaloxide/polymer nanocomposite films based on poly-ε-caprolactone and terephthalic acid, *Materials Science and Engineering C-Materials for Biological Applications*, **70**, **85-93,** (**2017**).
DOI: https://doi.org/10.1016/j.msec.2016.08.053
[12] A. Biundo, A. Hromic, T. Pavkov-Keller, K. Gruber, F. Quartinello, K. Haernvall, et al., Characterization of a poly(butylene adipate-co-terephthalate)- hydrolyzing lipase from Pelosinus fermentans, *Appl Microbiol Biotechnol*, **100**, **1753-1764,** (**2016**).
DOI: https://doi.org/10.1007/s00253-015-7031-1
[13] V. Perz, A. Baumschlager, K. Bleymaier, S. Zitzenbacher, A. Hromic, G. Steinkellner, et al., Hydrolysis of synthetic polyesters by Clostridium botulinum esterases, *Biotechnol Bioeng*, **113**, **1024-34,** (**2016**).
DOI: https://doi.org/10.1002/bit.25874
[14] I. E. Meyer Cifuentes, P. Wu, Y. Zhao, W. Liu, M. Neumann-Schaal, L. Pfaff, et al., Molecular and Biochemical Differences of the Tandem and Cold-Adapted PET Hydrolases Ple628 and Ple629, Isolated From a Marine Microbial Consortium, *Front Bioeng Biotechnol*, **10**, **930140,** (**2022**).
DOI: https://doi.org/10.3389/fbioe.2022.930140
[15] P. Svoboda, M. Dvorackova and D. Svobodova, Influence of biodegradation on crystallization of poly (butylene adipate-co-terephthalate), *Polymers for Advanced Technologies*, **30**, **552-562,** (**2019**).
DOI: https://doi.org/10.1002/pat.4491
[16] X. Jia, K. Zhao, J. Zhao, C. Lin, H. Zhang, L. Chen, et al., Degradation of poly(butylene adipate-co-terephthalate) films by *Thermobifida fusca* FXJ-1 isolated from compost, *Journal of Hazardous Materials*, **441**, (**2023**).
DOI: https://doi.org/10.1016/j.jhazmat.2022.129958

[17] A. Chorolque, C. Pozzo Ardizzi, G. Pellejero, G. Aschkar, F. J. García Navarro and R. Jiménez Ballesta, Incidence of bacterial diseases associated with irrigation methods on onions (Allium cepa), *J Sci Food Agric*, **98**, **5534-5540,** (**2018**).
DOI: https://doi.org/10.1002/jsfa.9101
[18] H. Wang, D. F. Wei, A. N. Zheng and H. N. Xiao, Soil burial biodegradation of antimicrobial biodegradable PBAT films, *Polymer Degradation and Stability*, **116**, **14-22,** (**2015**).
DOI: https://doi.org/10.1016/j.polymdegradstab.2015.03.007
[19] S. Yoshida, K. Hiraga, T. Takehana, I. Taniguchi, H. Yamaji, Y. Maeda, et al., A bacterium that degrades and assimilates poly(ethylene terephthalate), *Science*, **351**, **1196-1199,** (**2016**).
DOI: https://doi.org/10.1126/science.aad6359
[20] X. Han, W. D. Liu, J. W. Huang, J. T. Ma, Y. Y. Zheng, T. P. Ko, et al., Structural insight into catalytic mechanism of PET hydrolase, *Nature Communications*, **8**, (**2017**).
DOI: https://doi.org/10.1038/s41467-017-02255-z
[21] C. C. Chen, X. Han, X. Li, P. C. Jiang, D. Niu, L. X. Ma, et al., General features to enhance enzymatic activity of poly(ethylene terephthalate) hydrolysis, *Nature Catalysis*, **4**, **425-430,** (**2021**).
DOI: https://doi.org/10.1038/s41929-021-00616-y
[22] T. Fecker, P. Galaz-Davison, F. Engelberger, Y. Narui, M. Sotomayor, L. P. Parra, et al., Active Site Flexibility as a Hallmark for Efficient PET Degradation by *I-sakaiensis* PETase, *Biophysical Journal*, **114**, **1302-1312,** (**2018**).
DOI: https://doi.org/10.1016/j.bpj.2018.02.005
[23] K. E. Jaeger and T. Eggert, Lipases for biotechnology, *Current Opinion in Biotechnology*, **13**, **390-397,** (**2002**).
DOI: https://doi.org/10.1016/s0958-1669(02)00341-5
[24] P. Bracco, N. van Midden, E. Arango, G. Torrelo, V. Ferrario, L. Gardossi, et al., Bacillus subtilis Lipase A—Lipase or Esterase?, *Catalysts*, **10**, (**2020**).
DOI: https://doi.org/10.3390/catal10030308
[25] F. Muroi, Y. Tachibana, P. Soulenthone, K. Yamamoto, T. Mizuno, T. Sakurai, et al., Characterization of a poly(butylene adipate-oterephthalate) hydrolase from the aerobic mesophilic bacterium *Bacillus pumilus*, *Polymer Degradation and Stability*, **137**, **11-22,** (**2017**).
DOI: https://doi.org/10.1016/j.polymdegradstab.2017.01.006
[26] N. Wierckx, M. A. Prieto, P. Pomposiello, V. de Lorenzo, K. O'Connor and L. M. Blank, Plastic waste as a novel substrate for industrial biotechnology, *Microbial Biotechnology*, **8**, **900-903,** (**2015**).
DOI: https://doi.org/10.1111/1751-7915.12312
[27] R. A. Wilkes and L. Aristilde, Degradation and metabolism of synthetic plastics and associated products by *Pseudomonas sp.*: capabilities and challenges, *Journal of Applied Microbiology*, **123**, **582-593,** (**2017**).
DOI: https://doi.org/10.1111/jam.13472
[28] W. J. Li, T. Narancic, S. T. Kenny, P. J. Niehoff, K. O'Connor, L. M. Blank, et al., Unraveling 1,4-Butanediol Metabolism in *Pseudomonas putida* KT2440, *Frontiers in Microbiology*, **11**, (**2020**).
DOI: https://doi.org/10.3389/fmicb.2020.00382
[29] P. Liu, T. Zhang, Y. Zheng, Q. Li, Q. Liang and Q. Qi, Screening and genome analysis of a Pseudomonas stutzeri that degrades PET monomer terephthalate, *Acta Microbiologica Sinica*, **62**, **200-212,** (**2022**).
DOI: https://doi.org/10.13343/j.cnki.wsxb.20210178

[30] P. Liu, Y. Zheng, Y. B. Yuan, T. Zhang, Q. B. Li, Q. F. Liang, et al., Valorization of Polyethylene Terephthalate to Muconic Acid by Engineering *Pseudomonas Putida*, *International Journal of Molecular Sciences*, **23**, (**2022**).
DOI: https://doi.org/10.3390/ijms231910997
[31] M. Hao, W. Hui, L. Shao, C. Shi, F. Lu and H. Zhang, Improving the Ability of Bacilluslicheniformisto Produce Alkaline Protease by Inactivating Sec Pathway Repressor Protein and Extracellular Proteases, *China Biotechnology*, **44**, **39-47,** (**2024**).
DOI: https://doi.org/10.13523/j.cb.2307018
[32] J. de Keyzer, C. van der Does and A. J. M. Driessen, The bacterial translocase: a dynamic protein channel complex, *Cellular and Molecular Life Sciences*, **60**, **2034-2052,** (**2003**).
DOI: https://doi.org/10.1007/s00018-003-3006-y
[33] U. Canosi, G. Morelli and T. A. Trautner, The relationship between molecular structure and transformation efficiency of some S. aureus plasmids isolated from B. subtilis, *Molecular & general genetics : MGG*, **166**, **259-67,** (**1978**).
DOI: https://doi.org/10.1007/bf00267617
[34] S. M. Satti and A. A. Shah, Polyester-based biodegradable plastics: an approach towards sustainable development, *Letters in Applied Microbiology*, **70**, **413-430,** (**2020**).
DOI: https://doi.org/10.1111/lam.13287
[35] Z. Jiang, X. Chen, H. Xue, Z. Li, J. Lei, M. Yu, et al., Novel polyurethane-degrading cutinase BaCut1 from Blastobotrys sp. G-9 with potential role in plastic bio-recycling, *Journal of Hazardous Materials*, **472**, (**2024**).
DOI: https://doi.org/10.1016/j.jhazmat.2024.134493
[36] L. Sumbalova, J. Stourac, T. Martinek, D. Bednar and J. Damborsky, HotSpot Wizard 3.0: web server for automated design of mutations and smart libraries based on sequence input information, *Nucleic Acids Res*, **46**, **W356-w362,** (**2018**).
DOI: https://doi.org/10.1093/nar/gky417
[37] Y. Joho, V. Vongsouthi, C. Gomez, J. S. Larsen, A. Ardevol and C. J. Jackson, Improving plastic degrading enzymes via directed evolution, *Protein Eng Des Sel*, **37**, (**2024**).
DOI: https://doi.org/10.1093/protein/gzae009
[38] T. Bayer, L. Pfaff, Y. Branson, A. Becker, S. Wu, U. T. Bornscheuer, et al., Biosensor and chemo-enzymatic one-pot cascade applications to detect and transform PET-derived terephthalic acid in living cells, *iScience*, **25**, **104326,** (**2022**).
DOI: https://doi.org/10.1016/j.isci.2022.104326
[39] Y. Qiao, R. Hu, D. Chen, L. Wang, Z. Wang, H. Yu, et al., Fluorescence-activated droplet sorting of PET degrading microorganisms, *J Hazard Mater*, **424**, **127417,** (**2022**).
DOI: https://doi.org/10.1016/j.jhazmat.2021.127417
[40] Y. Z. Wang, Y. Zhou and G. J. Zylstra, Molecular analysis of isophthalate and terephthalate degradation by Comamonas testosteroni YZW-D, *Environ Health Perspect*, **103 Suppl 5**, **9-12,** (**1995**).
DOI: https://doi.org/10.1289/ehp.95103s49
[41] H. R. Schläfli, M. A. Weiss, T. Leisinger and A. M. Cook, Terephthalate 1,2-dioxygenase system from Comamonas testosteroni T-2: purification and some properties of the oxygenase component, *J Bacteriol*, **176**, **6644-52,** (**1994**).
DOI: https://doi.org/10.1128/jb.176.21.6644-6652.1994
[42] K. Y. Choi, D. Kim, W. J. Sul, J. C. Chae, G. J. Zylstra, Y. M. Kim, et al., Molecular and biochemical

analysis of phthalate and terephthalate degradation by Rhodococcus sp. strain DK17, *FEMS Microbiol Lett*, **252**, **207-13,** (**2005**).
DOI: https://doi.org/10.1016/j.femsle.2005.08.045
[43] P. Liu, Y. Zheng, Y. Yuan, T. Zhang, Q. Li, Q. Liang, et al., Valorization of Polyethylene Terephthalate to Muconic Acid by Engineering Pseudomonas Putida, *Int J Mol Sci*, **23**, (**2022**).
DOI: https://doi.org/10.3390/ijms231910997
[44] H. Hara, D. Eltis Lindsay, E. Davies Julian and W. Mohn William, Transcriptomic Analysis Reveals a Bifurcated Terephthalate Degradation Pathway in Rhodococcus sp. Strain RHA1, *J Bacteriol*, **189**, **1641-1647,** (**2007**).
DOI: https://doi.org/10.1128/jb.01322-06
[45] S. M. Miller, T. Wang and D. R. Liu, Phage-assisted continuous and non-continuous evolution, *Nature protocols*, **15**, **4101-4127,** (**2020**).
DOI: https://doi.org/s41596-020-00410-3
[46] H. S. Kim, M. H. Noh, E. M. White, M. V. Kandefer, A. F. Wright, D. Datta, et al., Biocomposite thermoplastic polyurethanes containing evolved bacterial spores as living fillers to facilitate polymer disintegration, *Nat Commun*, **15**, **3338,** (**2024**).
DOI: https://doi.org/10.1038/s41467-024-47132-8
[47] C. Zeng, F. Ding, J. Zhou, W. Dong, Z. Cui and X. Yan, Biodegradation of Poly(ethylene terephthalate) by *Bacillus safensis* YX8, *International Journal of Molecular Sciences*, **24**, (**2023**).
DOI: https://doi.org/10.3390/ijms242216434
[48] G. M. Morris, R. Huey, W. Lindstrom, M. F. Sanner, R. K. Belew, D. S. Goodsell, et al., AutoDock4 and AutoDockTools4: Automated docking with selective receptor flexibility, *Journal of computational chemistry*, **30**, **2785-2791,** (**2009**).
DOI: https://doi.org/10.1002/jcc.21256

Acknowledgments

We are grateful to the support of Nanjing Agricultural University (NAU). We sincerely thank professor Xin Yan and professor Xi Chen for providing materials and their advice.

Author contributions

Y.X. and L.R.J. conceived and designed the project, H.C.Y., L.K.X., Y.C.H., H.W.Y., L.R.J. performed experiments with support from Z.M.L., L.J., Y.Y.X. and L.Y.; H.C.Y., L.R.J., Y.C.H., L.K.X., H.W.Y., Y.Y.X. and Z.M.L. wrote the article with contributions from other authors; B.J.X. and M.R.Y. provided some figures in the article; Z.X.H. accounted for the computational experiments. C.X. and Y.X. agree to serve as corresponding authors and ensures communication.

Competing interests

The authors declare no competing interests.

Supplementary information is available for this paper in the online version.